CGU HS Committee on River Ice Processes and the Environment
13th Workshop on the Hydraulics of Ice Covered Rivers
Hanover, NH, September15-16, 2005

Numerical Modeling of Storage Release during Dynamic River Ice Break-up

Martin Jasek
BC Hydro, Burnaby, BC, Canada, martin.jasek@bchydro.com

George Ashton
Lebanon, NH, USA, george.ashton@valley.net

Hung Tao Shen and Fanghui Chen
Clarkson University, Potsdam, NY, USA, htshen@clarkson.edu, chenf@clarkson.edu

The stage of an ice-covered river is higher than the stage without an ice cover. As break-up progresses downstream, the release of the ice cover results in release of the storage associated with the ice cover. Approximate calculations suggest this storage release could amplify the arriving hydrograph, but it is unclear whether this storage release adds to the peak of the hydrograph or merely lengthens the hydrograph.

This paper describes numerical simulations using the unsteady one-dimensional river ice model of CRISSP (Comprehensive River Ice Simulation System Program) to simulate break-up in a rectangular channel. Model runs were conducted for different pre-break-up (base) discharges, break-up initiating discharge and channel bed slopes to determine the effects of these parameters on the features of the discharge wave that propagates downstream. Specifically, the question whether or not this discharge-wave could amplify and/or self-sustain itself is addressed for various conditions.

1.0 Introduction

BC Hydro owns and operates the W.A.C. Bennett and Peace Canyon dams on the Peace River in northern British Columbia. The company is continuing investigations into the effects of regulation and environmental conditions on ice-jam formation so that the river can be managed more effectively. The water released from channel storage could have significant effect on break-up on the Peace River as well as secondary consolidation events during freeze-up but the effects are poorly understood.

Channel storage release results when an ice cover starts to move (break-up), its resistance to flow underneath diminishes and due to the increase in conveyance the stage drops and the extra water contributes to the discharge in the river. How exactly this extra water is incorporated into the overall river flow has not been studied in much detail but the mechanism has been suspect in causing break-up fronts to sustain long advances, Jasek (2003).

2.0 Field Data and Previous Studies

There seems to have been little work on the effect of storage release on break-up hydrographs. Prowse and Carter (1998) estimated the storage release contribution to the break-up hydrograph on the Mackenzie River to be as much as 25% during the freshet period but did not detail how the hydrograph was changed. Ashton (2003) suggested that the storage release effect on the Peace River could contribute as much as 1650 m^3/s to the break-up hydrograph based on a simple computation of the storage release associated with a front celerity of 170 km/day.

Break-up fronts observed on large northern rivers have been documented to travel at great speeds over large distances. For example, Gerard et al. (1984) observed on the Yukon River a break-up front that traveled about 300 kilometres at an average rate of about 5.2 m/s.

Beltaos (2003) presented a theoretical formulation for the onset of mechanical river break-up. Its basis was the lifting of the ice sheet by a stage increase that allows room for the ice sheets to start moving around bends and obstacles. A prerequisite to this was some longitudinal and transverse cracking preceding break-up (which is often observed in the field) that would allow the ice to move as separate units. Once moving, the large ice sheets would fracture rapidly into smaller ones. The onset of break-up was formulated as a function of a certain stage rise, the maximum freeze-up ice elevation, the pre break-up ice thickness and strength, which were a function of thermal deterioration from the maximum winter ice thickness and strength. Site specific constants dependent on channel curvature and river width were also involved.

Ferrick and Mulherin (1989) conducted numerical simulations for discharge waves that triggered break-up of an ice cover based on exceeding a certain stress value at the side hinge cracks. A one-dimensional unsteady-flow hydraulic model that solved the open channel flow continuity equations (with an allowance for an ice cover) using the Preissman or four-point implicit finite difference method (Cunge et al., 1980) was employed. Their findings indicated that if the ice cover did not break-up, the rates of stage and discharge increase as well as the wave amplitude would diminish with downstream distance. However, if a break-up front was triggered by the wave, the numerical simulations indicated that the rate of discharge and stage rise were greater than for the non-break-up case and that the peak discharge could amplify in the downstream direction. The wave also traveled faster than in the non-break-up case. The authors suggested

that these results emphasized the importance of the release of water from storage during break-up that counteracted wave attenuation. The simulations were conducted for the Connecticut River over a length of about 20 km with river widths typically between 100 and 200 m, and a mean bed slope of 0.00037. Due to the relative short river reach it could not be concluded from this study if this mechanism could explain the sustained high break-up front celerities on large northern rivers over 100s of kilometers.

Once a break-up front is in motion, Jasek (2003) went on to describe two types of break-up fronts based on field observations, sheet fronts and rubble fronts. The former occurred in rivers where the ice was more free to move either due to channel geometry or low strength and thickness while the latter in more confined channels with stronger ice.

3.0 CRISSP 1D

CRISSP1D is a comprehensive state-of-the-art ice simulation model for use by hydroelectric utilities and others concerned with river ice issues. The technology addresses both the design and operational issues including the development of procedures for establishing favorable ice formation conditions in the early ice formation period as well as the establishment of operating policies compatible with ice conditions and which will contribute to the maximization of the productivity of generation stations. The model is applicable to a wide range of hydraulic engineering needs, including ice jam related flood analysis studies, applications to wintertime navigation and transportation, climate change studies, and ice related environmental and ecological studies. The model is able to simulate river ice processes and associated flow conditions. The ice processes include water temperature and ice concentration distributions of suspended and surface ice, ice cover formation, progression, and consolidation, undercover transport and accumulation, ice jam evolution, thermal growth and decay of ice cover including the effect of a snow cover, cover stability, initiation of break-up, breakup ice run and jam. Specific features of the models include the ability of treating river networks, transitional flows, and internal hydraulic structures

In CRISSP1D the four-point implicit model for river networks developed by Potok and Quinn (1979) is used for solving the St.Venant equations for flow hydraulics. Calculation of ice properties are calculated separately using an Eulerian-Lagrangian technique at a smaller time step than the hydraulics calculation. The two calculations were coupled at every hydraulics time step.

CRISSP1D has several empirical mechanisms for handling break-up. The option that was used in this study was a discharge criterion; if a discharge exceeds a certain critical value, the ice cover is broken.

Since CRISSP1D does not include the dynamic interactions of ice pieces in the surface ice run, it allows the user to specify a higher bed roughness as a function of surface ice concentration (for ice runs) to reflect the extra flow resistance from bumping and grinding of the ice pieces. The Manning's n for the bed increases from the open water condition starting at a certain threshold ice concentration ($Cc = 0.6$) and increases exponentially to a higher Manning's n at maximum ice concentration of $Ccmax = 0.9$.

4.0 Methodology

Initially, numerical simulations were set up for two rectangular channels one with a bed slope of 0.0003 and the other with a bed slope of 0.00005 with lengths of 500 km and 1000 km, respectively. Both were 600 m wide. Two additional simulations were conducted for a 100 m wide channel with a slope of 0.0003 and a length of 500 km. The cross section spacings were 1 km for the 500 km channels and 2 km for the 1000 km channel. The hydraulics time step was either 10 or 20 minutes depending on the channel bed slope with milder slopes using the latter. . The ice calculation time step was 1/40 of the hydraulics time step in this study. A 0.7 m thick ice cover was placed on the lower 400 km portion and lower 800 km portion of the 500 km and 1000 km long channels respectively. The bed roughness and the under ice roughness were given a Manning's n value of 0.03. The higher roughness for the latter was to simulate solid ice that had undergone some thermal deterioration causing rippling of the ice underside. The domains were initialized to a steady-state discharge of 1600 m^3/s.

Rather than considering any one or more of the complex theoretical formulations or whether the break-up front was of the sheet or rubble variety (as outlined in Section 2) for specifying when break-up would occur in the CRISSP1D simulations, the simple discharge threshold option was used. The rational behind this was that since the channel was prismatic and since the initial ice thickness was the same everywhere, many of the stage and strength based criteria would be exceeded for the same discharge at any point along the channel. Thus the break-up initiating discharge (Q_{break}) was used in this study. Thermal inputs that would cause time varying ice thickness were "turned-off" in the simulations.

Discharge waves of various magnitudes and duration were introduced at the upstream boundary condition and allowed to propagate downstream towards the ice cover and further downstream. The discharge wave was given as a triangular distribution with the rising limb 3 times steeper than the falling limb. If a discharge wave was greater than the break-up initiating discharge for the ice cover then the ice cover would fail and cause a break-up front to continue downstream as long as the discharge was above the threshold value. The downstream boundary condition consisted of a solid floating ice cover rating curve consistent with the initial ice cover that was present in the channel.

5.0 Results

5.1 Typical Results

Figure 1 shows the discharge contours plotted vs. distance and time for a non-break-up case. The discharge wave slows down as it reaches the ice cover and attenuates in the downstream direction. Figure 2 shows that same discharge wave at the upstream boundary condition but in this simulation the break-up discharge of 2400 m^3/s is exceeded at the leading edge of the ice cover by only 30 m^3/s. This caused a break-up front to commence from the leading edge and release water from storage and the discharge wave to amplify for 100 km downstream to a value of about 3750 m^3/s. The value attenuated slightly but approached a self-sustaining value of about 3640 m^3/s for another 300 km. In the first 100 km the break-up front traveled at 5.2 m/s and in the last 300 km it traveled at 3.8 m/s. This appears to be in the order of that observed by Gerard et al. (1984) in terms of celerity and distance traveled. This is in contrast with the depth

averaged water velocity (Figure 3) which was 1.5 m/s and 0.8 m/s upstream and downstream of the break-up front respectively. The shape of the break-up wave (Figure 4) shows that its abrupt rise from 3.96 m to 4.83 m is maintained at the break-up front for hundreds of kilometres but its crest is flat and its duration increases. Figures 5 and 6 show the surface ice concentration and surface ice discharge respectively indicating that ice run is increasing in length with time as expected. High ice concentration coincides with high stage and high total discharge.

Figure 7 shows the longitudinal water surface and bottom of stationary ice profiles for different times for the same Run 9. The figure shows that the shape of the front of discharge wave is maintained at the break-up front, akin to a kinematic wave. However, unlike the kinematic wave the celerity is much greater than 1.5 times the water velocity (Ponce and Simons, 1977). In this case the factor is 2.5 (from Figure 3).

5.2 Effect of Base Discharge and Break-up initiating discharge

Figure 8 shows three plots of discharge vs. distance and time for different break-up initiating discharges and the same base flow (Q_{base}). In Figure 8a the ratio of Q_{break}/Q_{base} is close to 1, essentially the entire river is just on the verge of break-up. The resulting break-up front celerity (C_{br}) is very high at 9.1 m/s. In Figure 8b, Q_{break}/Q_{base} is 1.5 and C_{br} = 3.8 m/s and in Figure 8c Q_{break}/Q_{base} is 2.0 and C_{br} = 3.3 m/s. Thus it appears that the closer the base flow is to the break-up initiating discharge, the faster a self-sustaining break-up front will travel.

5.3 Effect of Wave Duration

Figure 2 and Figure 8b show two simulations with the same Q_{break} and Q_{base} but with a wave duration of 18 hours and 4 days respectively. In the first 100 km of the two simulations, C_{br} was equal 5.7 m/s and 7.2 m/s respectively. It appears that the broader wave initiated a faster break-up front initially. However, from 300 to 500 km C_{br} had reached a constant value of 3.8 m/s for both simulations.

5.4 Effect of Bed Slope

Figure 9a and 9b shows a simulation for a smaller bed slope of 0.00005 compared to simulations presented thus far, which were for a bed slope of 0.0003 (See Figure 8b for comparison). A surprising result of these smaller slope simulations was that the break-up stalled about 10 km upstream of the end of the channel. The reason for this has not been investigated fully but it could be the result of the imperfect downstream boundary condition, which is a steady-state rating curve for the ice cover. For such a mild channel, the rating curve during discharge wave events would be expected to be strongly looped. Thus forcing the steady-state rating curve at the downstream boundary condition may have caused the discharge to become less than Q_{break} and stopped the break-up process. The arriving ice from upstream then accumulated to form a jam indicated by the high total depths in Figure 9b. This does not invalidate the run in terms of looking at the break-up front as the jamming occurred later.

Figure 9 (for S = 0.00005) can be compared to Figure 8b (for S =0.0003) which have the same Q_{break}/Q_{base} ratio of 1.5. The break-up front celerities are slightly less for the milder channel.

Figure 10 shows results for S = 0.00005 and a Q_{break}/Q_{base} ratio of 2.0 which is comparable to Figure 8c with S = 0.0003. In this case C_{br} is significantly smaller for the milder channel, 2.6 m/s vs. 3.3 m/s.

Figure 11 shows results for S = 0.00005 and a Q_{break}/Q_{base} ratio of 1.01, which is comparable to Figure 8a with S = 0.0003. In this case C_{br} is significantly larger for the milder channel, 11.8 m/s vs. 9.1 m/s.

5.5 Effect of Increasing Bed Roughness with Ice Concentration in the Ice Run

The results presented thus far specified no increase in the Manning's n for the bed (Bman2) with ice concentration. The same is true for Figure 12a where Bman2 = 0.03 = bed roughness and under-ice roughness. Figure 12b and 12c shows the effect of increasing Bman2 to 0.04 and 0.05 respectively. Values higher than 0.05 (although simulated) would be unreasonable, as they would produce depths that are higher than the stationary ice cover. The results show that the C_{br} slows down with an increase in Bman2 as expected. With no increase in bed roughness (Bman2 = 0.03), C_{br} = 3.8 m/s, for Bman2 = 0.04, C_{br} = 3.4 m/s and for Bman2 = 0.05, C_{br} = 3.3 m/s.

The use of Bman2 to account for ice dynamics is empirical and there are no studies on what value should be selected. However, Figure 12c shows that Bman2 = 0.05 is probably too high for this case since it pushes the high discharge portion of the ice run to the upstream end of it which does not look reasonable. This is even the case for Bman2 = 0.04 (Figure 12b) although not so extreme. Figure 13 shows the depths for the Bman2 = 0.04 case and shows a very high and sharply defined stage peak (5.7 m) at the tail end of the ice run compared to 4.7 m at the downstream end and middle of the ice run. This is generally not found in the field and indicates that even Bman2 = 0.04 may be too high.

5.5 Effect of Channel Width

Figure 14 shows a simulation for a narrow channel of 100 m but with the same bed slope and unit discharge as the 600 m wide channel in Figure 2. The break-up front celerities and discharge patterns were nearly identical for the two runs indicating that channel width does not have much of an effect on the break-up front or ice run, at least not in rectangular channels. C_{br} in the first 100 km was only 0.1% lower, the self-sustaining C_{br} from 200 to 500 km was 1.9% lower and $Q_{sustained}/Q_{base}$ was 2.6% lower.

5.6 Summary of Runs

Table 1 summarizes the input parameters (first 10 columns) for runs conducted in this study. Output features of the runs are noted in the last 6 columns of Table 1. The first of these is the Discharge at the leading edge, which is the maximum discharge that arrives at the leading edge of the ice cover that triggers break-up (if break-up is permitted), usually slightly higher than Q_{break}. $Q_{sustained}$ is the self-sustaining discharge just upstream of the breaking front in the region of $C_{br\ sustained}$. $C_{br\ 100km}$ is the break-up front celerity in the first 100 km and $C_{br\ sustained}$ is the break-up front celerity in the latter $^3/_5{}^{th}$ of the channel where it has reached a constant value. The last two columns are ratios of discharges already described.

Table 1. Summary of CRISSP runs and results

Run #	Bed Slope	Channel Width (m)	Q_{base} (m^3/s)	Q_{break} (m^3/s)	Q_{peak} (m^3/s)	Wave Duration	Bman1	Bman2	Ice Manning	Q at leading edge (m^3/s)	Q sustained (m^3/s)	C_{br} 100km (m/s)	C_{br} sustained (m/s)	Q_{break}/Q_{base}	Q_{sus}/Q_{base}
1	0.0003	600	1600	no break-up	1800	3 hours	0.03	0.03	0.03	1631					
2	0.0003	600	1600	1620	1800	3 hours	0.03	0.03	0.03	1631	2900	9.1	9.1	1.01	1.81
3	0.0003	600	1600	no break-up	3400	4 days	0.03	0.03	0.03	3260					
4	0.0003	600	1600	3200	3400	4 days	0.03	0.03	0.03	3260	4300	5.9	3.3	2.00	2.69
5	0.0003	600	1600	no break-up	2600	4 days	0.03	0.03	0.03	2430					
6	0.0003	600	1600	2400	2600	4 days	0.03	0.03	0.03	2430	3600	7.2	3.8	1.50	2.25
7	0.0003	600	1600	2400-4000	2600	4 days	0.03	0.03	0.03	2430					
8	0.0003	600	1600	no break-up	3000	18 hours	0.03	0.03	0.03	2430					
9	0.0003	600	1600	2400	3000	18 hours	0.03	0.03	0.03	2430	3640	5.2	3.8	1.50	2.28
10	0.0003	600	1600	2400	3000	18 hours	0.03	0.06	0.03	2430	2500	3.8	3.0	1.50	1.56
11	0.0003	600	1600	2400	3000	18 hours	0.03	0.04	0.03	2430	3090	4.4	3.4	1.50	1.93
12	0.0003	600	1600	2400	3000	18 hours	0.03	0.05	0.03	2430	2650	4.1	3.3	1.50	1.66
13	0.0003	600	1600	2400	3000	18 hours	0.03	0.07	0.03	2430	2400	3.5	2.7	1.50	1.50
14	0.0003	600	1600	2400	3000	18 hours	0.03	0.08	0.03	2430	2400	2.7	2.0	1.50	1.50
15	0.0003	600	1600	no break-up	2100	4 days	0.03	0.03	0.03	2055					
16	0.0003	600	1600	2000	2100	4 days	0.03	0.03	0.03	2055	3350	5.7	4.6	1.25	2.09
b1	0.0005	600	1600	no break-up	2100	6 hours	0.03	0.03	0.03	1629					
b2	0.0005	600	1600	1620	2100	6 hours	0.03	0.03	0.03	1629	2670	11.8	11.8	1.01	1.67
b3	0.0005	600	1600	no break-up	4600	4 days	0.03	0.03	0.03	3230					
b4	0.0005	600	1600	3200	4600	4 days	0.03	0.03	0.03	3230	3530	6.7	2.6	2.00	2.21
b5	0.0005	600	1600	no break-up	3600	4 days	0.03	0.03	0.03	2673					
b6	0.0005	600	1600	2400	3600	4 days	0.03	0.03	0.03	2673	3000	6.8	3.7	1.50	1.88
b7	0.0005	600	1600	2400-4000	3600	4 days	0.03	0.03	0.03	2673					
b8	0.0005	600	1600	no break-up	8000	18 hours	0.03	0.03	0.03	2498					
b9	0.0005	600	1600	2400	8000	18 hours	0.03	0.03	0.03	2498	3000	4.7	3.8	1.50	1.88
c1	0.0003	100	267	no break-up	500	18 hours	0.03	0.03	0.03	402					
c2	0.0003	100	267	400	500	18 hours	0.03	0.03	0.03	402	593	5.2	3.8	1.50	2.22

6.0 Conclusions

Simulated break-up fronts using CRISSP 1D have indicated that self-sustaining break-up fronts are possible for long distances and travel at relatively high speeds consistent with observations on large northern rivers. In the first 100 km, the break-up front celerity is higher than the self-sustaining break-up front celerity further down the channel. Discharges amplify in the first 100 km, peak, diminish slightly and then reach a self sustaining value, the magnitude of which generally increases with river slope and the break-up initiating discharge. The self-sustaining discharge can be several times the base flow.

A sharp rise at the break-up front is maintained with distance traveled and the crest is flat and lengthens with distance as more ice is broken up. The long crest contains the region of the ice run.

The closer that a river is to breaking up (the closer Q_{break} is to Q_{base}), the faster the break-up front was found to travel. The differences can be significant and maximum values for Q_{break} / Q_{base} close to unity were 9.1 and 11.2 m/s for the 0.0003 and 0.00005 sloped channels respectively. It was only for values of Q_{break} / Q_{base} close to unity that the break-up front traveled faster for a milder channel. For higher Q_{break} / Q_{base} a milder channel had a slower break-up front celerity.

Broader waves that initiate break can cause the break-up front to travel faster initially but the self-sustaining break-up front celerity further down the channel appears to be independent of the triggering wave shape.

There was a larger difference in break-up front celerities between a higher sloped and lower sloped channels if the Q_{break} / Q_{base} ratio was higher.

Increasing the Manning's n coefficient for the bed in the region of the ice run to empirically model the ice dynamics slows down the break-up front slightly but causes the back end of the ice run to be higher in stage than the front and middle portion of the ice run.

Channel width did not effect the break-up front celerity and the ability of the storage release to sustain the break-up front.

Acknowledgments

CRISSP1D is a software for one-dimensional unsteady-state flow river hydraulics and ice calculations. It is a part of the software developed for the Comprehensive River ice Simulation Systems Project (CRISSP), which is supported by the Water Resource Management Interest Group (WMIG), CEA Technologies Inc. of the Canadian Electricity Association. CRISSP1D is a product of CEATI.

The CRISSP1D model was developed by the River Ice Research Group at Department of Civil and Environmental Engineering, Clarkson University, under the direction of Dr. Hung Tao Shen. Dr. Fanghui Chen was responsible for the programming of the new development in CRISSP1D

References

Ashton, G. D. 2003. Ice jam flooding on the Peace River near the Peace-Athabasca Delta, Canadian Water Resources Association 56th Annual Conference, 11-13 June 2003, Vancouver, BC, pp. 315-323.

Beltaos, S., 2003. Threshold condition between mechanical and thermal breakup. 12th Workshop on the Hydraulics of Ice Covered Rivers. Edmonton, AB.

Cunge, J. A., Holly, F.M. Jr., and Verway, A., 1980. Practical Aspects of Computational River Hydraulics, Pitman Pub. Inc., Marshfiled, Massachusetts, 62-96.

Gerard, R., T.D. Kent, R. Janowicz and R.O. Lyons., 1984. Ice regime reconnaissance, Yukon River, Yukon. Proceedings of the Cold Regions Engineering Specialty Conference, Canadian Society for Civil Engineering, Montreal, QC, pp. 1059-1073.

Jasek, M., 2003. Ice Jam Release Surges, Ice Runs and Breaking Fronts – Field Measurements, Physical Descriptions and Research Needs. Canadian Journal of Civil Engineering. Vol. 30, No. 1, pp. 113-127.

Ponce, V.M. and Simons, D.B. 1977. Shallow wave propagation in open channel flow. Journal of the Hydraulics Division, ASCE, 103(HY12), 1461-1476.

Potok, A.J., and Quinn, F.H., 1979. A Hydraulic Transient Model of the Upper St. Lawrence River for Water Resources Research, *Water Resources Bulletin*, 15(6).

Prowse, T. D. and Carter, T.., 2002. Significance of ice-induced storage to spring runoff: A case study of the Mackenzie River, Hydrol. Process., 16: 779-788.

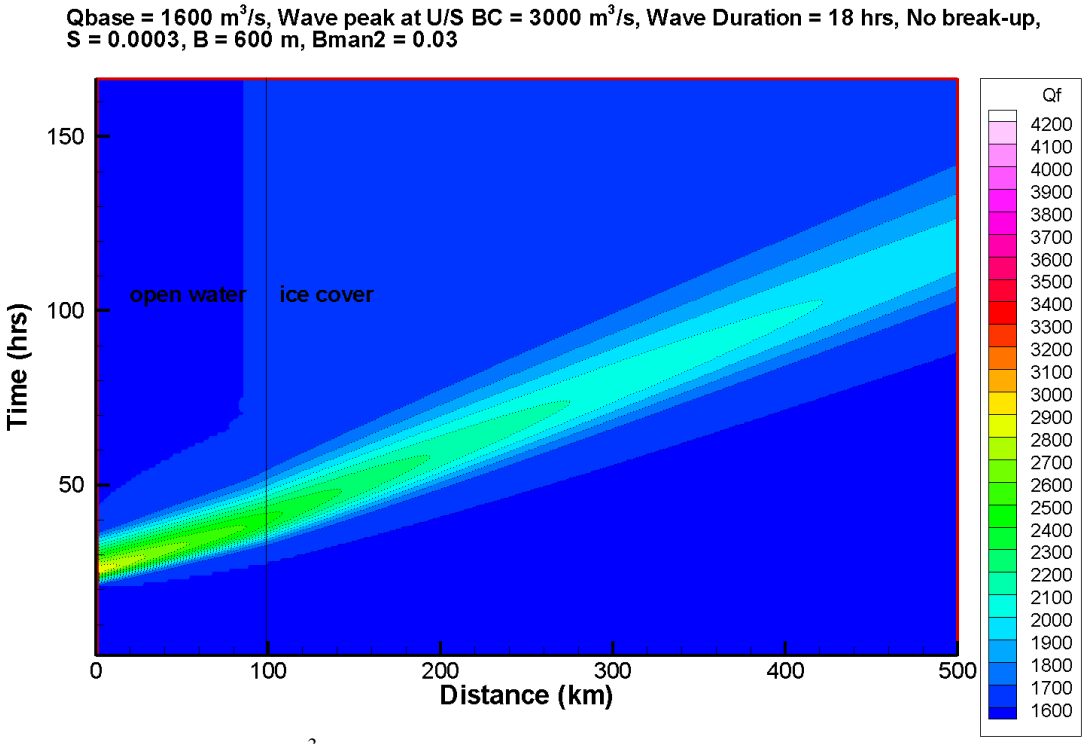

Figure 1. Discharge (m^3/s) vs. distance and time for non-break-up case, (Run 8).

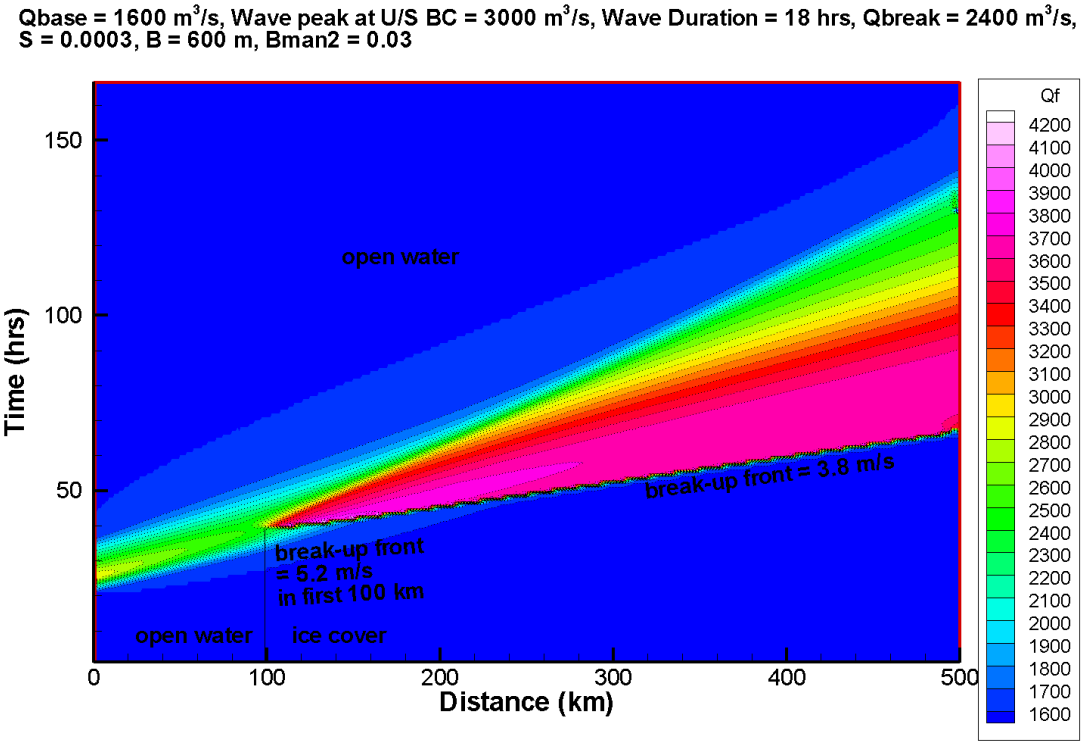

Figure 2. Discharge (m^3/s) vs. distance and time for break-up case (Run 9) with identical upstream discharge wave boundary condition as non break-up case Run 8 (Figure 1).

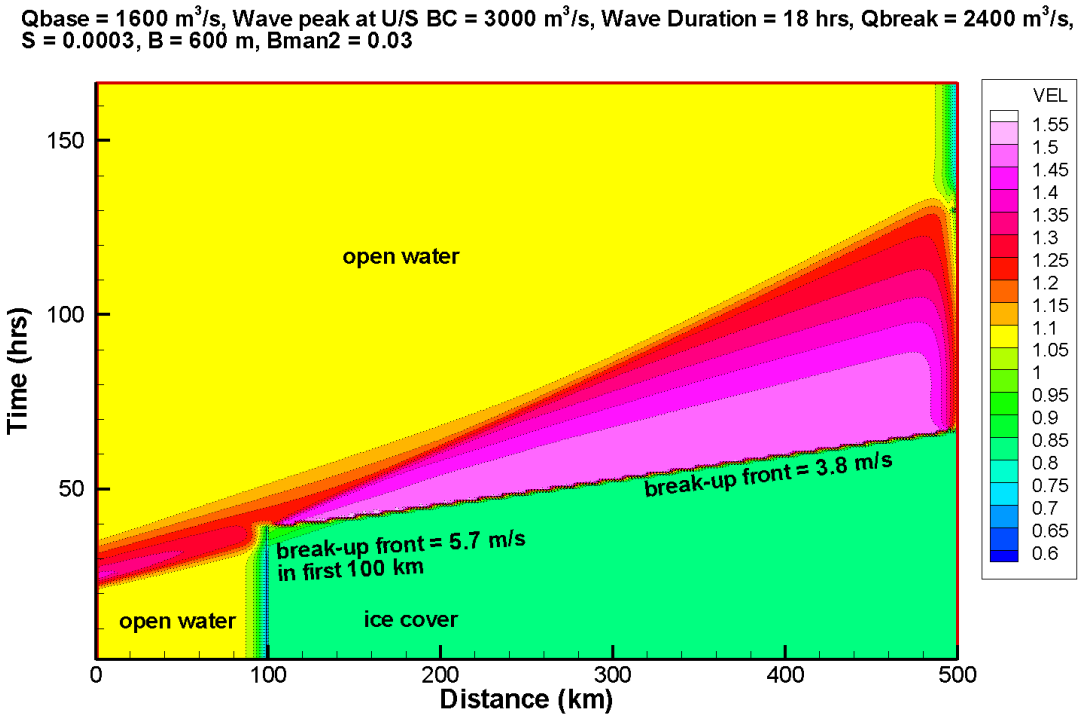

Figure 3. Mean velocity (m/s) vs. distance and time for break-up case (Run 9).

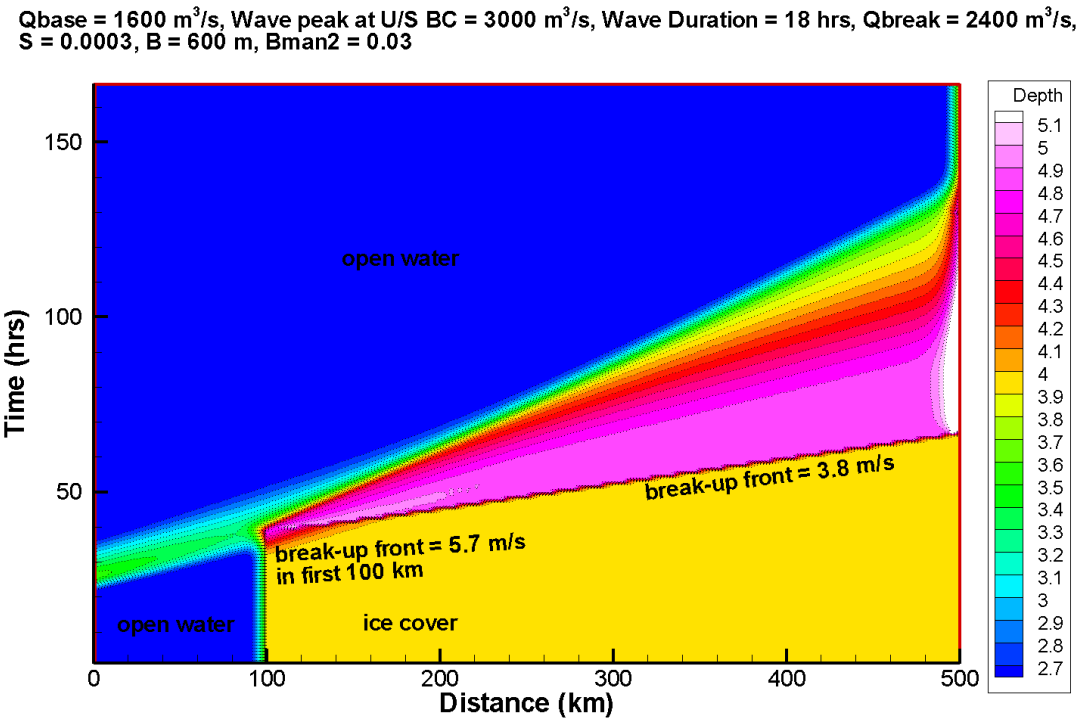

Figure 4. Total Depth (m) vs. distance and time for break-up case (Run 9).

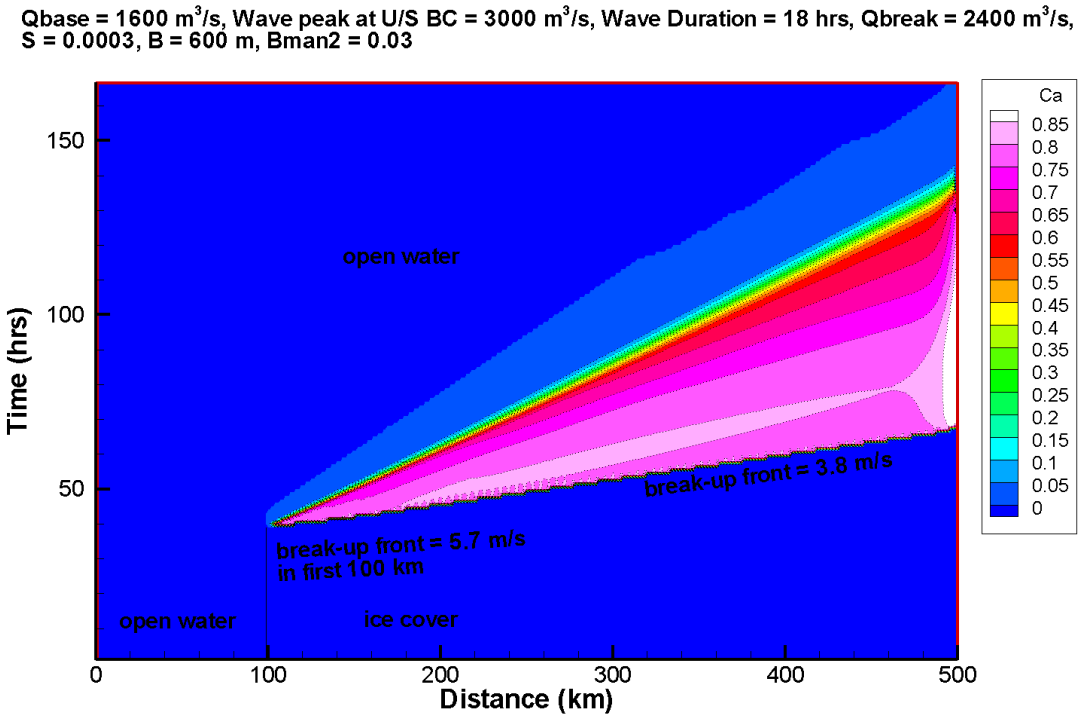

Figure 5. Surface ice concentration vs. distance and time for break-up case (Run 9). Maximum concentration in CRISSP set to 0.9.

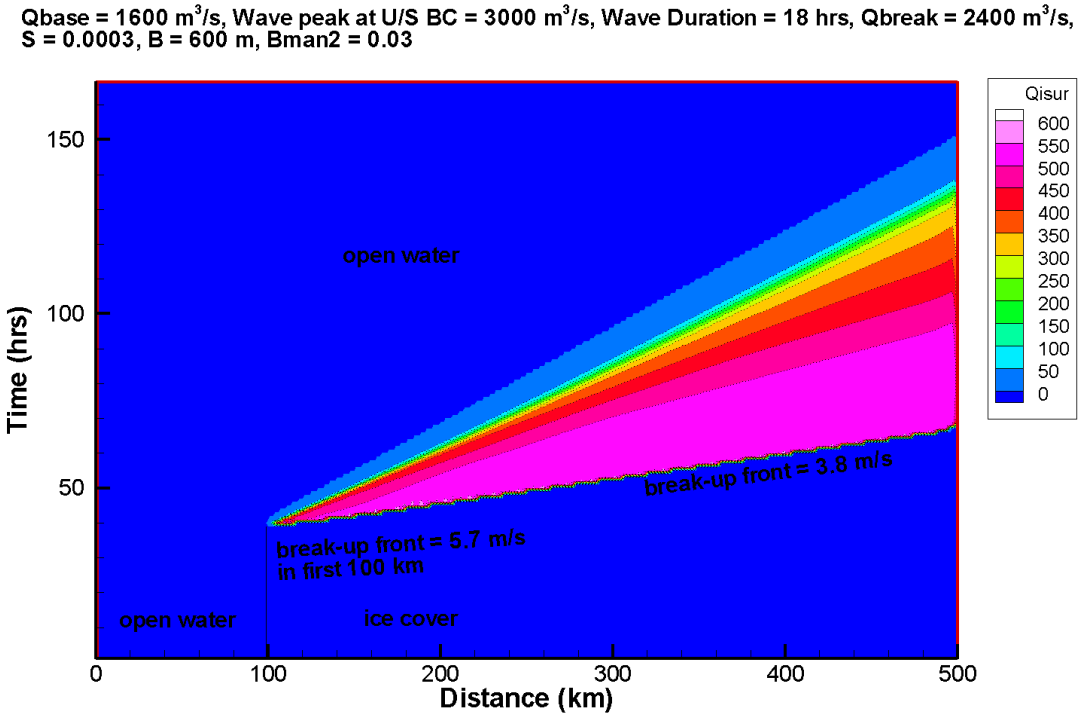

Figure 6. Surface ice discharge (m^3/s) vs. distance and time for break-up case (Run 9).

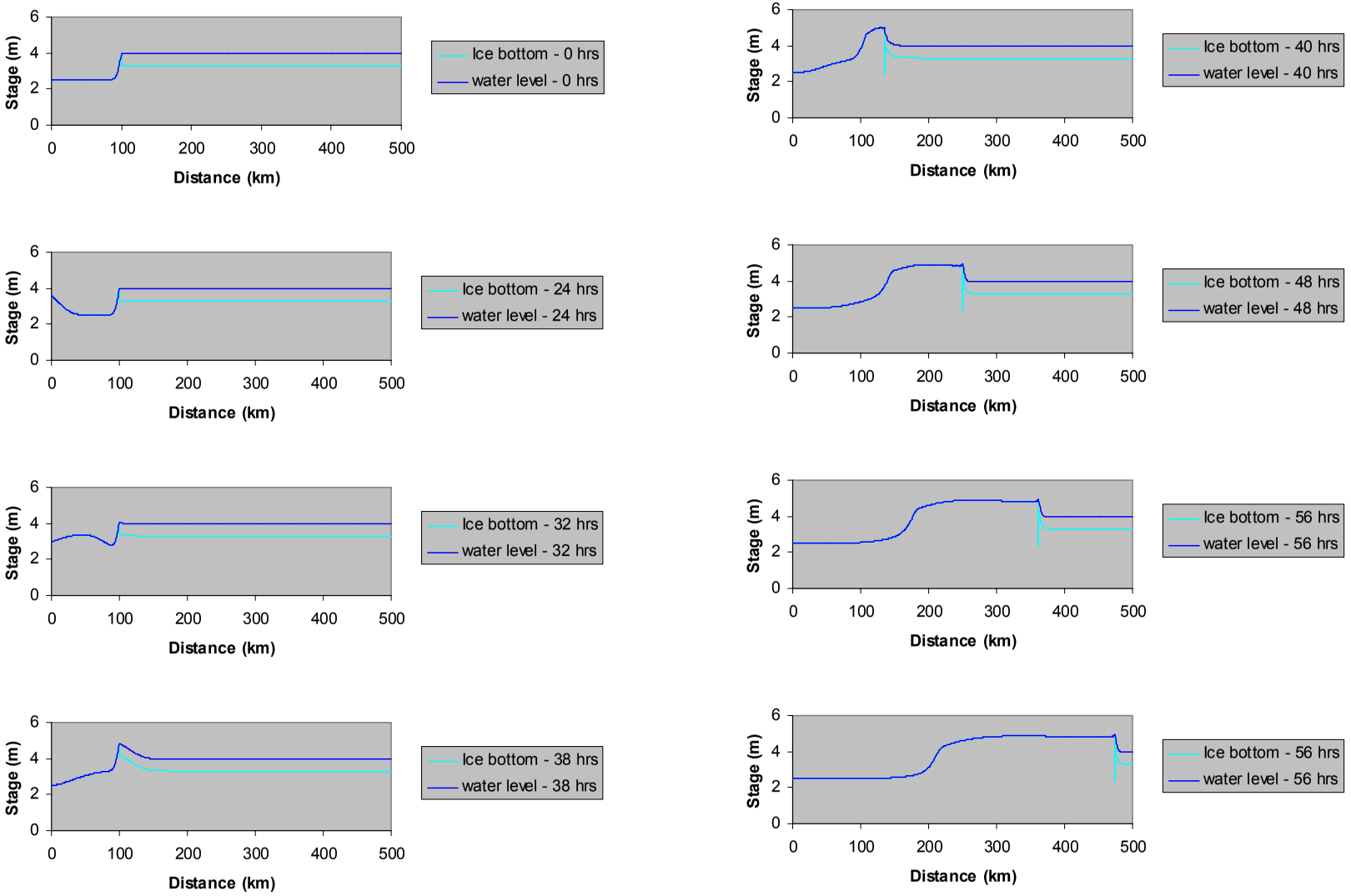

Figure 7. Simulated break-up (Run 9) showing storage release sustaining the break-up front for hundreds of kilometers. Moving ice in ice run is not shown but occupies the broad crest of the wave.

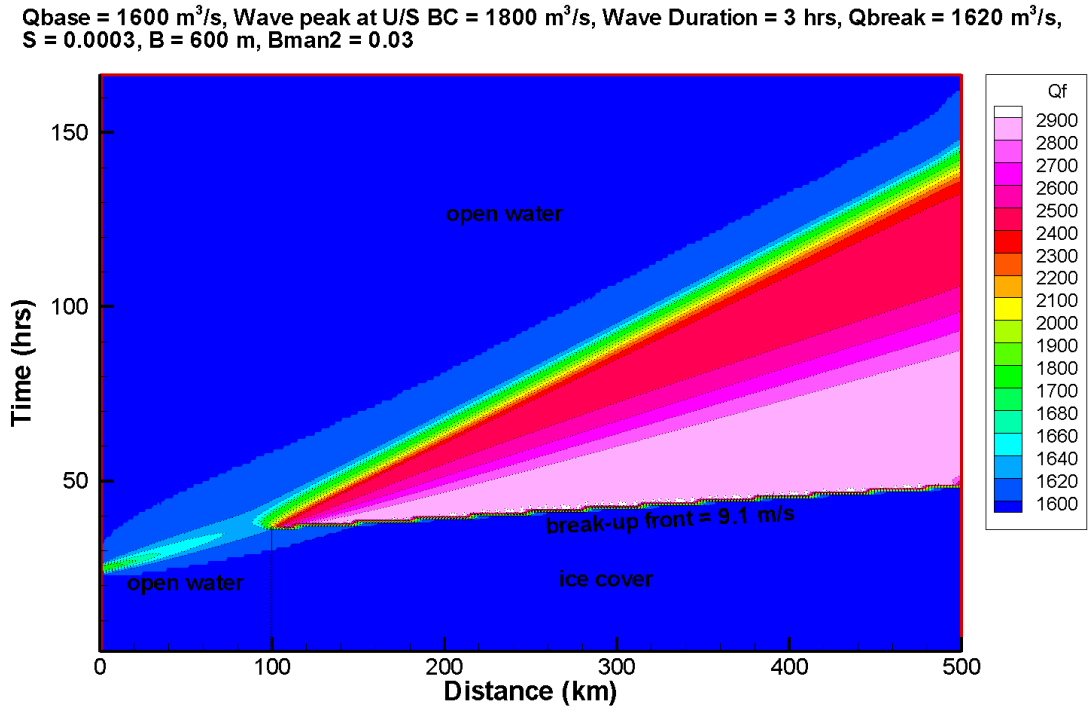

Figure 8a. Discharge (m^3/s) vs. distance and time for break-up case (Run 2). Break-up discharge (1620 m^3/s) only slightly higher than the base discharge (1600 m^3/s); Qbreak/Qbase = 1.01

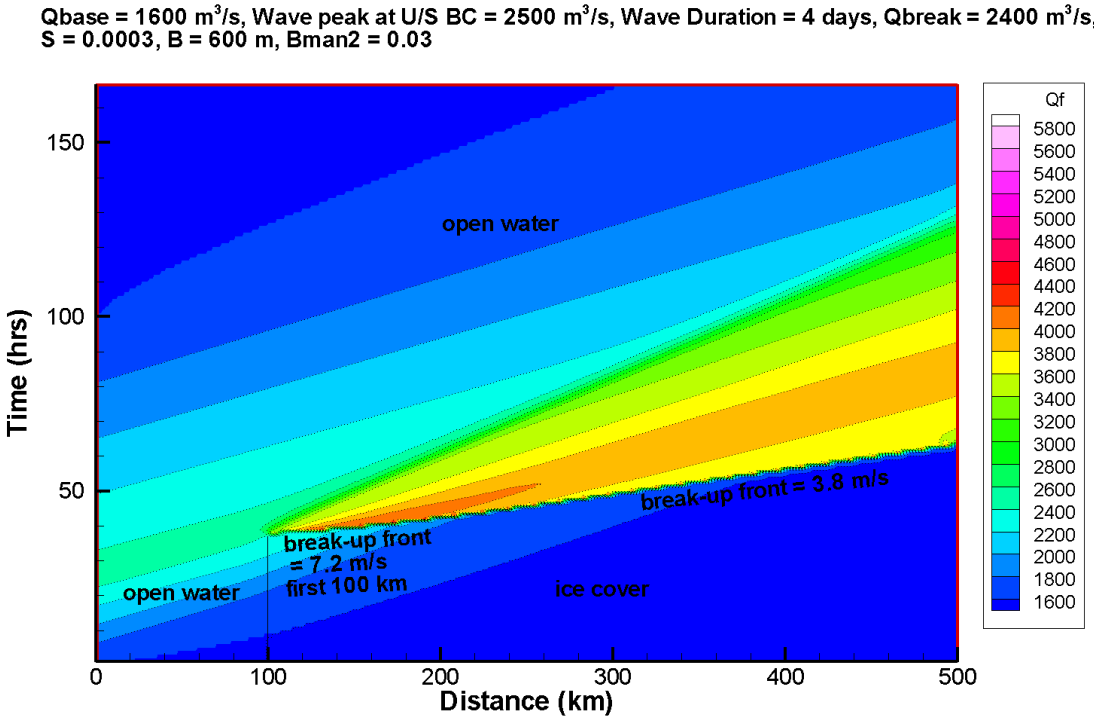

Figure 8b. Discharge (m^3/s) vs. distance and time for break-up case (Run 6). Break-up discharge (2400 m^3/s) base discharge (1600 m^3/s). Qbreak/Qbase = 1.5

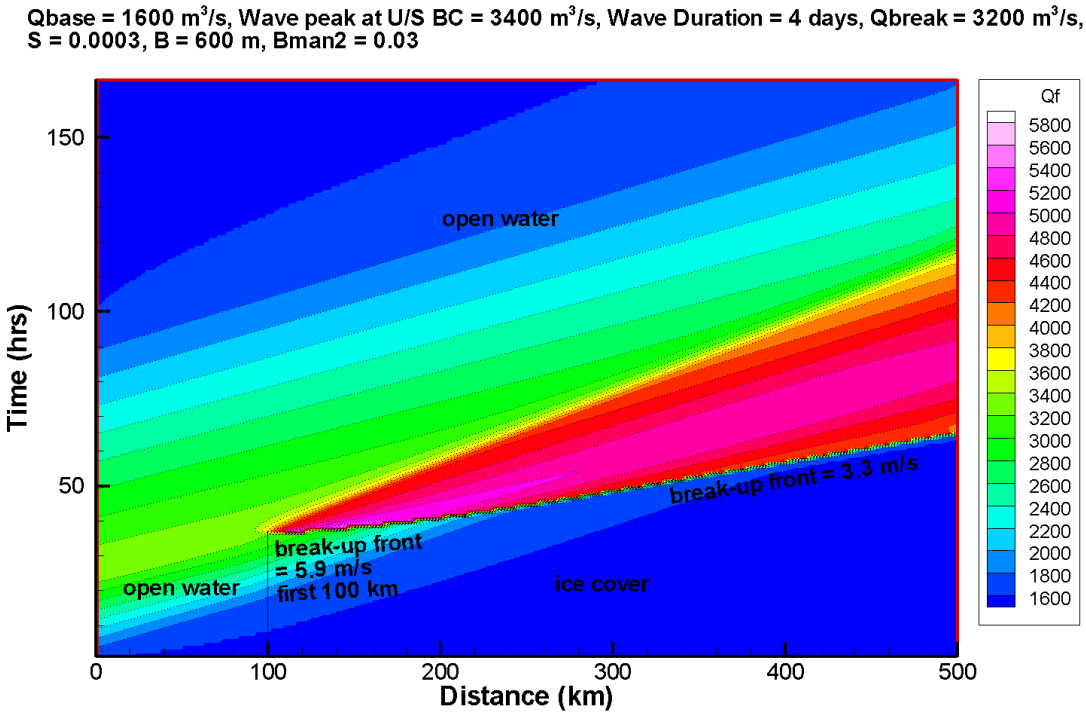

Figure 8c. Discharge (m^3/s) vs. distance and time for break-up case (Run 4). Break-up discharge (3200 m^3/s) base discharge (1600 m^3/s). Qbreak/Qbase = 2.0

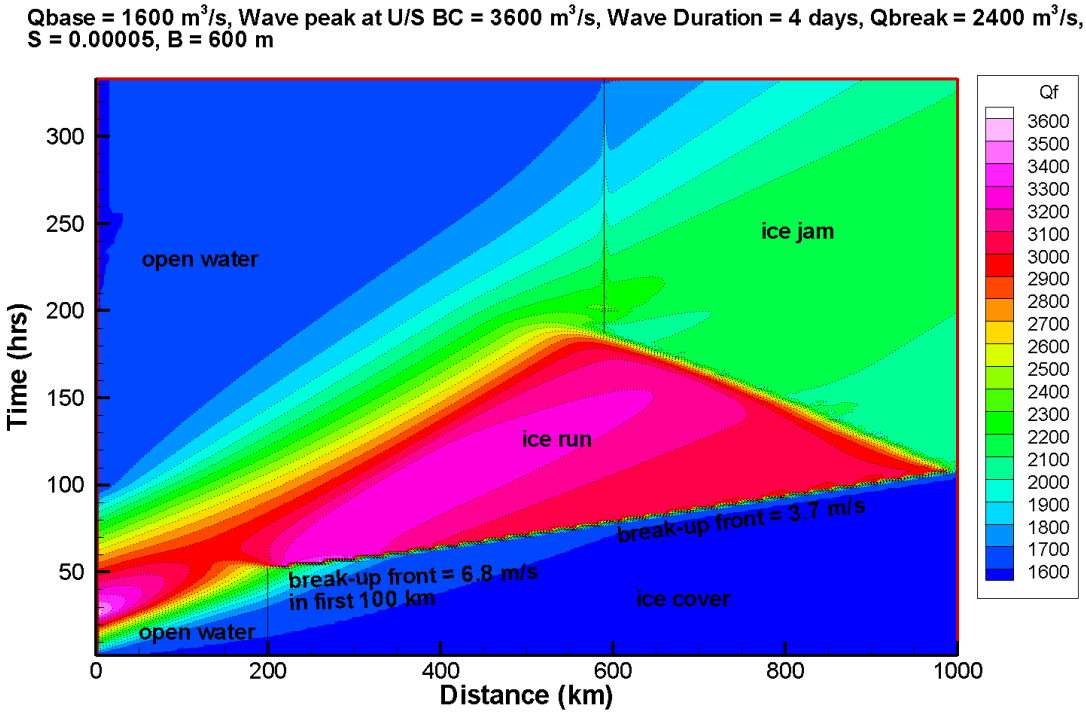

Figure 9a. Discharge (m^3/s) vs. distance and time for break-up case Run 6b. Qbreak/Qbase = 1.5.

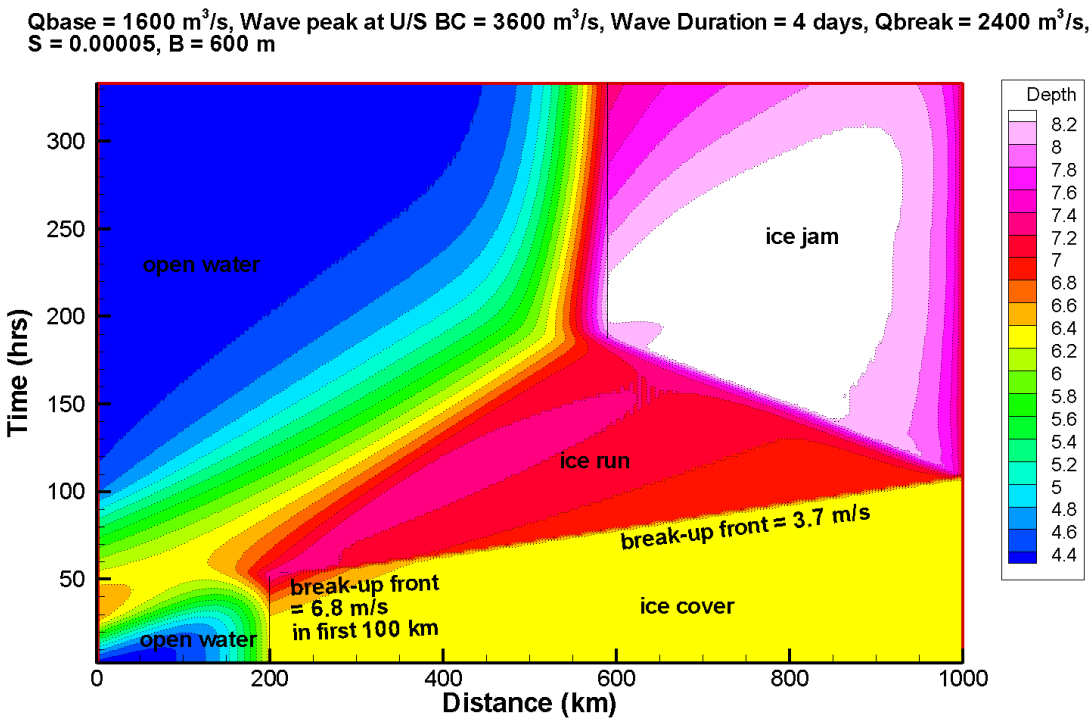

Figure 9b. Total Depth (m) vs. distance and time for break-up case Run 6b. Qbreak/Qbase = 1.5.

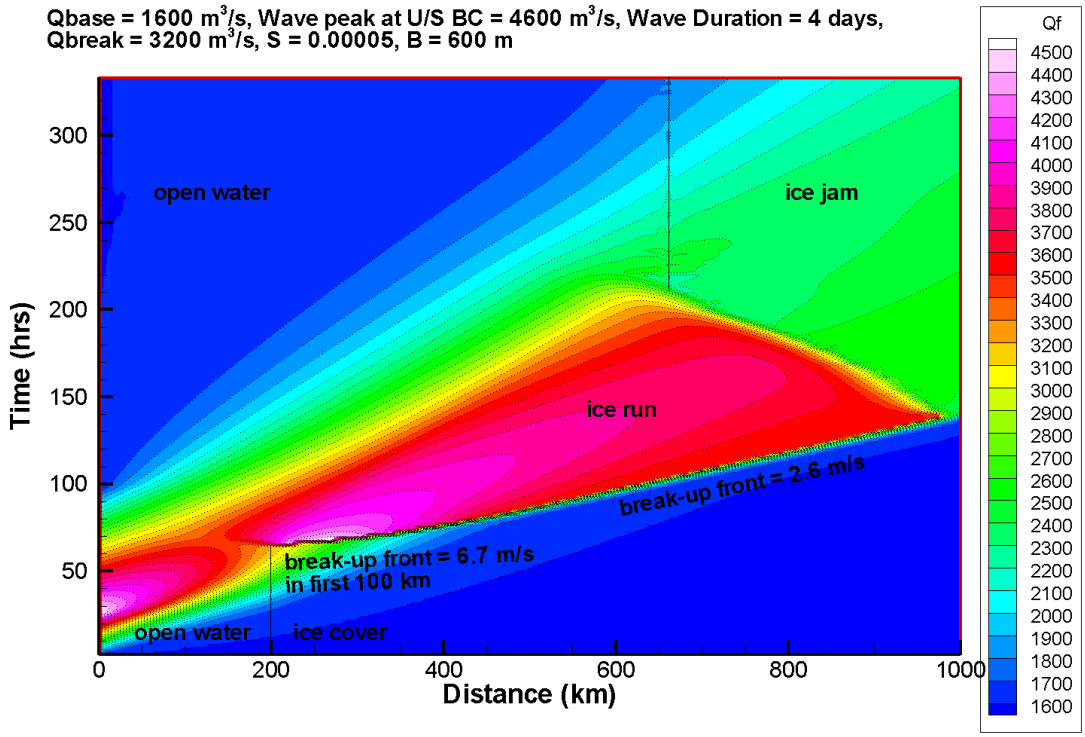

Figure 10. Discharge (m^3/s) vs. distance and time for break-up case Run 4b. Qbreak/Qbase = 2.0.

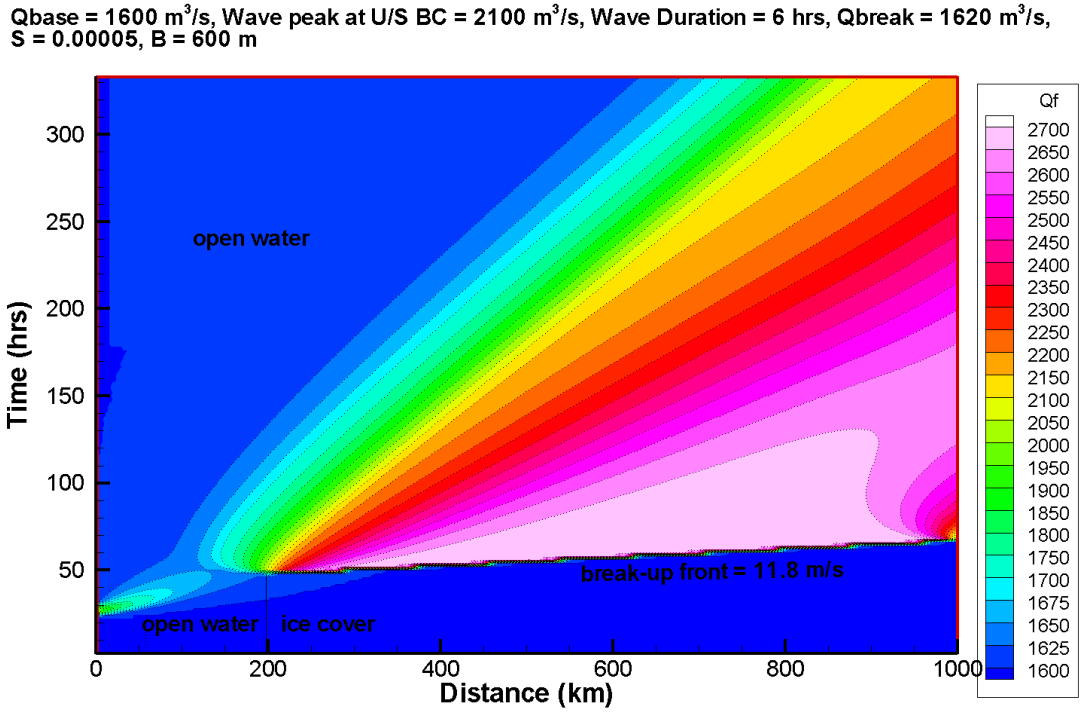

Figure 11. Discharge (m^3/s) vs. distance and time for break-up case Run 2b. Qbreak/Qbase = 1.01.

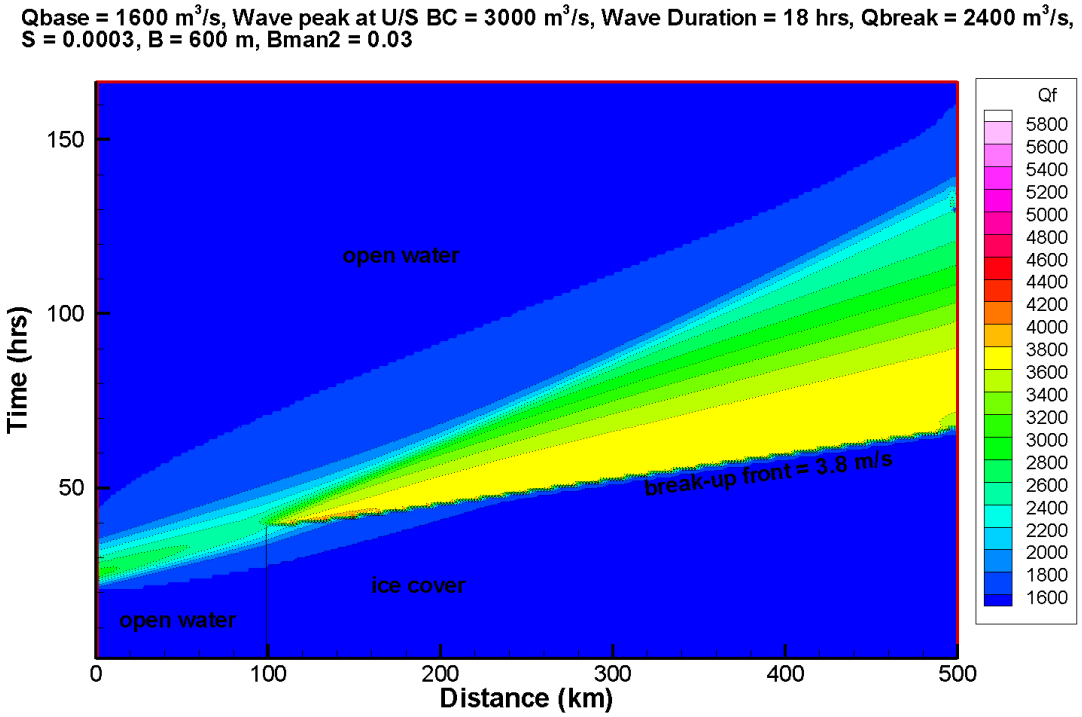

Figure 12a. Discharge (m^3/s) vs. distance and time for break-up case Run 9, Bman2 = 0.03.

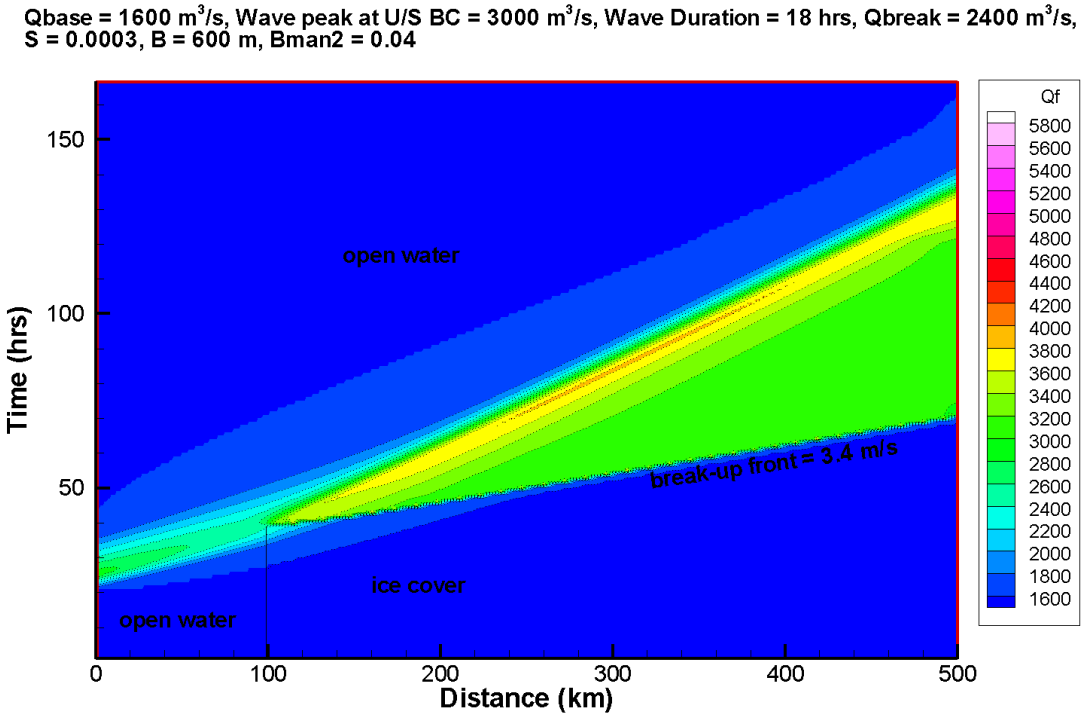

Figure 12b. Discharge (m^3/s) vs. distance and time for break-up case Run 11, Bman2 = 0.04.

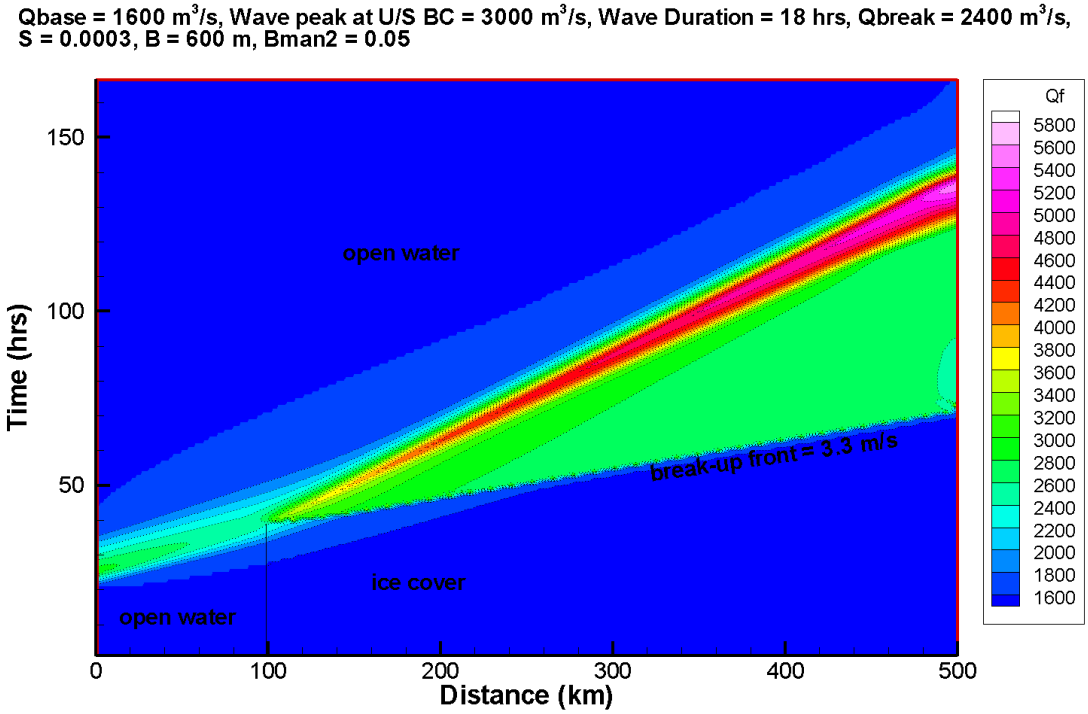

Figure 12c. Discharge (m^3/s) vs. distance and time for break-up case Run 12, Bman2 = 0.05.

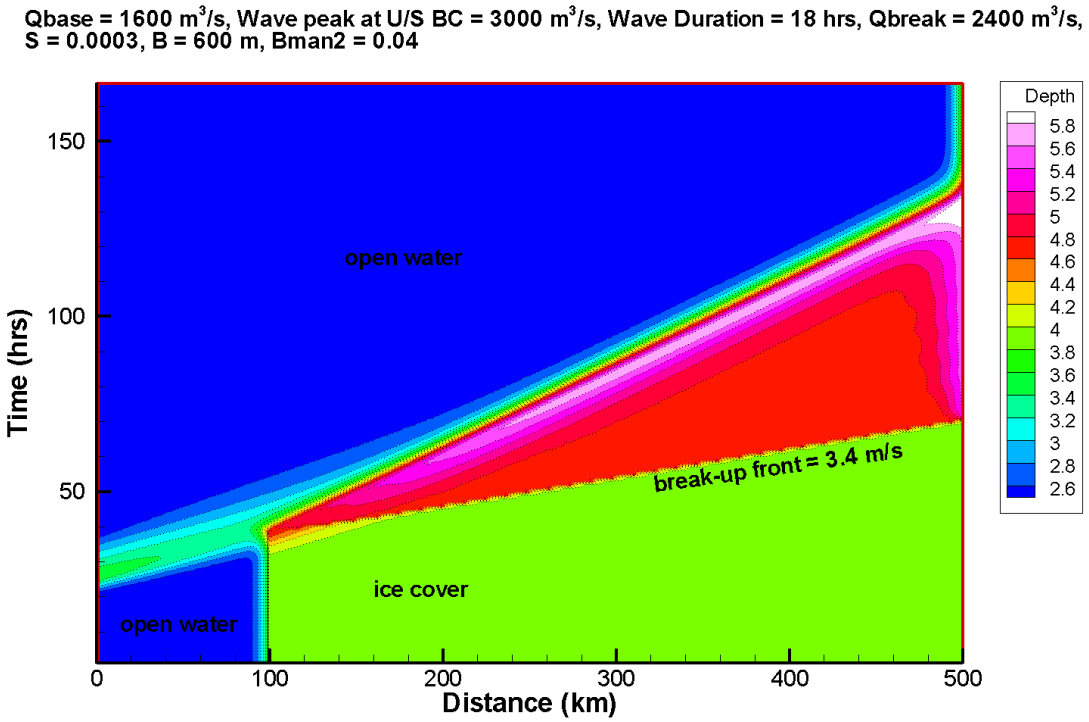

Figure 13. Depth (m) vs. distance and time for break-up case Run 11, Bman2 = 0.04.

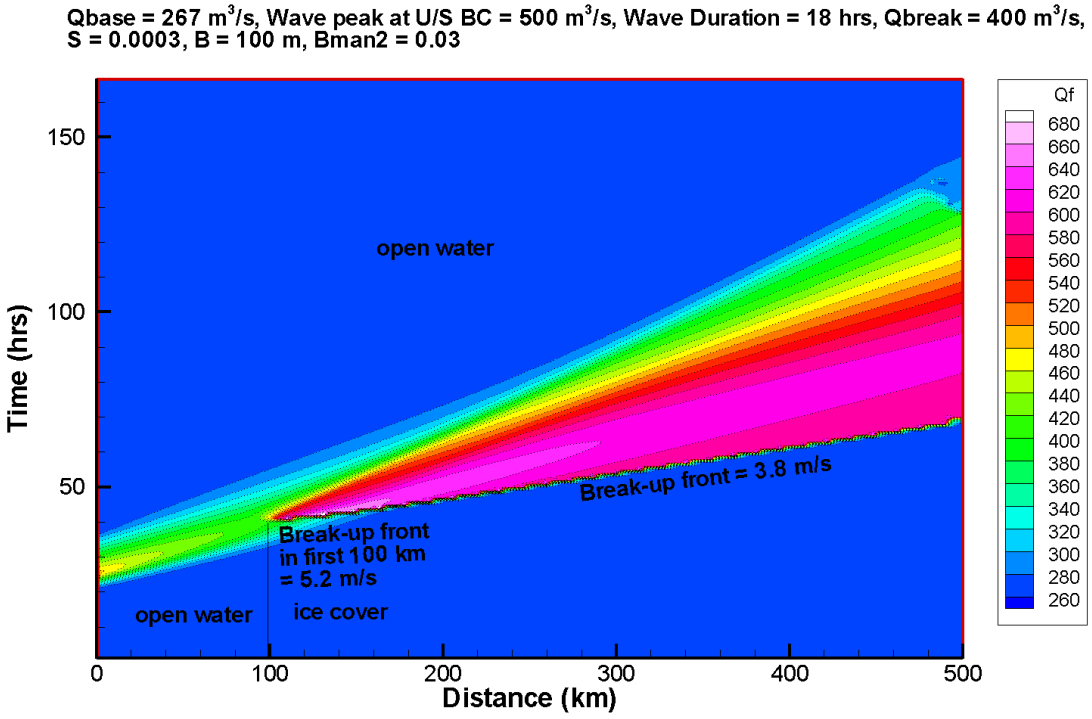

Figure 14. Discharge (m^3/s) vs. distance and time for break-up case Run 2c, for a narrow channel of 100 m with equivalent unit width discharge to 600 m wide channel in Run 9 Figure 2.